

Creep Behaviour of 316L Stainless Steel Srepared by 3D Printing

DYMÁČEK P.^{1,a}, KLOC L.^{1,b}, GABRIEL D.^{2,c}, MASÁK J.^{2,d}, PAGÁČ M.^{3,e},
HALAMA R.^{3,f}

¹Institute of Physics of Materials, Czech Academy of Sciences, Žitkova 22, 616 62 Brno, Czech Republic

²Institute of Thermomechanics, Czech Academy of Sciences, Dolejškova 1402/5 182 00 Praha, Czech Republic

³Faculty of Mechanical Engineering, VŠB – Technical University of Ostrava, 17. Listopadu 2172/15, 708 00 Ostrava, Czech Republic

^apdymacek@ipm.cz, ^bkloc@ipm.cz, ^cgabriel@it.cas.cz, ^dmasak@it.cas.cz
^emarek.pagac@vsb.cz, ^fradim.halama@vsb.cz

Keywords: 3D print, Selective laser melting, 316L Stainless steel, Creep

Abstract. The 3D printed 316L stainless steel produced by selective laser melting (SLM) was subjected to short term creep testing at 700 °C. Two directions of printing: i) horizontal and ii) vertical, were selected to test the creep performance of the steel. Comparison with the open literature data shows very good short-term creep properties of 3D printed steel that are superior to conventional steel. Both studied directions of printing show similar results so the steel can be considered from creep point of view as isotropic. The solution annealing prior to the creep testing slightly, but not substantially, lowers the creep performance of the steel.

Introduction

The 3D printing by selective laser melting (SLM) is a prospective method of metal powder consolidation and offers enormous possibilities for parts production. The mechanical behaviour of SLM prepared samples such as static, fatigue and creep properties has been intensively studied recently [1,2]. The necessity of experiments for a phenomenological description of fatigue, creep or creep-fatigue interaction behaviour in technical practice is evident [3,4] to perform reliable numerical analysis in various industries [5].

The short term creep behaviour at 700 °C of 316L cylindrical samples produced in horizontal and vertical direction by SLM technology is the subject of this study.

Material and testing

The technology of additive manufacturing usually named as Selective Laser Melting was used for the production of 3D printed 316L samples. The principle lies in the application of thin layers of a powdery material, which, according to the STL (an abbreviation of "stereolithography") model, are sintered with one laser beam layer after layer. The most important parameters of 3D print process set in Renishaw AM400 were: laser power 200 W, scanning speed 650 mm/s, exposure time 80 µs, focus size (laser beam diameter) 80 µm, layer thickness 50 µm, strategy Meander.

With respect to the orientation of the parts in the construction chamber, support material was designed to eliminate residual stresses and thermal distortion. When finishing 3D printing, the 316L steel has a Ra surface roughness of 5 to 10 μm [6]. Material for finishing operations by machining was added to the wall of the sample to achieve the desired surface roughness and manufacturing tolerances. The samples were scanned by the Meander strategy, which is characterized by a higher melting rate, and after each created layer, the scan direction is rotated by 67° . This controlled rotation ensures that the scanned laser trajectories of each successive layer are not identical. The chemical composition of the powder is shown in Table 1.

Table 1: Chemical composition of 316L powder in wt. %

| Chem. Comp. | C | Cr | Ni | Mo | Mn | Si | N | O | P | S | Fe |
|-------------|-------|-------|-------|-----|------------|------------|------------|------------|-------------|-------------|-------|
| % | <0.02 | 16–18 | 10–14 | 2–3 | ≤ 1.0 | ≤ 1.0 | ≤ 0.1 | ≤ 0.1 | ≤ 0.04 | ≤ 0.03 | ball. |

The steel was 3D printed in the form of cylinders ($d = 12 \text{ mm}$, $L = 75 \text{ mm}$) as shown in Fig. 1. Eight specimens were produced for each direction. After 3D print one group of cylinders for each direction was left in an as received while the second one was solution annealed at 1150°C for 10 min. Subsequently cylindrical specimens with M10 threaded heads ($d_{\text{gauge}} 6 \text{ mm}$, $L_{\text{gauge}} 35 \text{ mm}$) were produced from 3D printed cylinders.

Optical micrographs of microstructure taken by Olympus GX51 Inverted Metallographic Microscope in bright field at $100\times$ magnification are shown in Fig. 2. The arrows indicate the cylindrical specimen axial direction. The grinding and polishing with OP-S colloidal silica followed by electro-etching (10 V, 45 s) in 10% oxalic acid was applied for the metallographic surface preparation. Orientation of the layers for the two different building directions is clearly visible in as received specimens. The weld pool boundaries have fully dissolved after solution annealing. Some grains resemble twins but there is need of more detailed analysis of the microstructure by scanning microscope techniques. Some cavities of size between $20\text{--}200 \mu\text{m}$ are visible and some of them contain powder particles.

The specimens were crept in lever arm creep testing machines in Ar protective atmosphere at 700°C and 120, 160 and 200 MPa stress in constant load conditions.

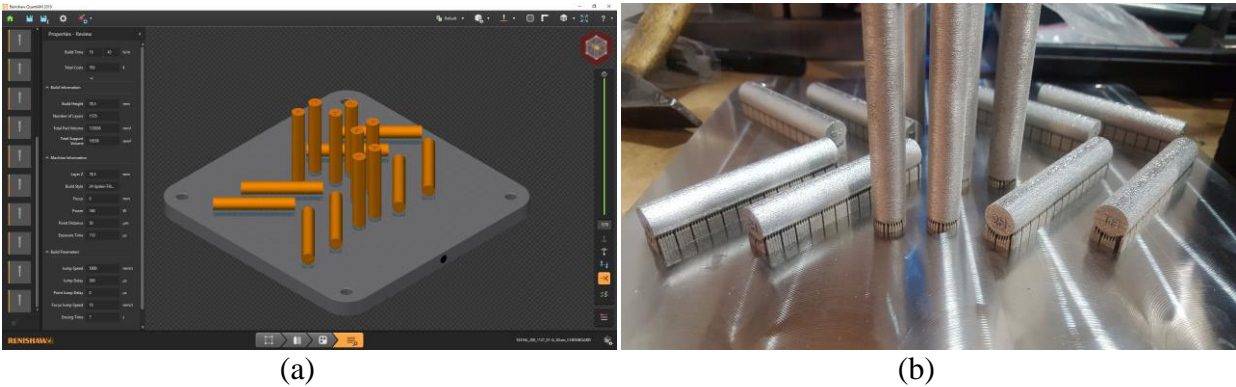


Fig. 1: Specimen layout (a) in the printing software (b) after printing on the supporting bed

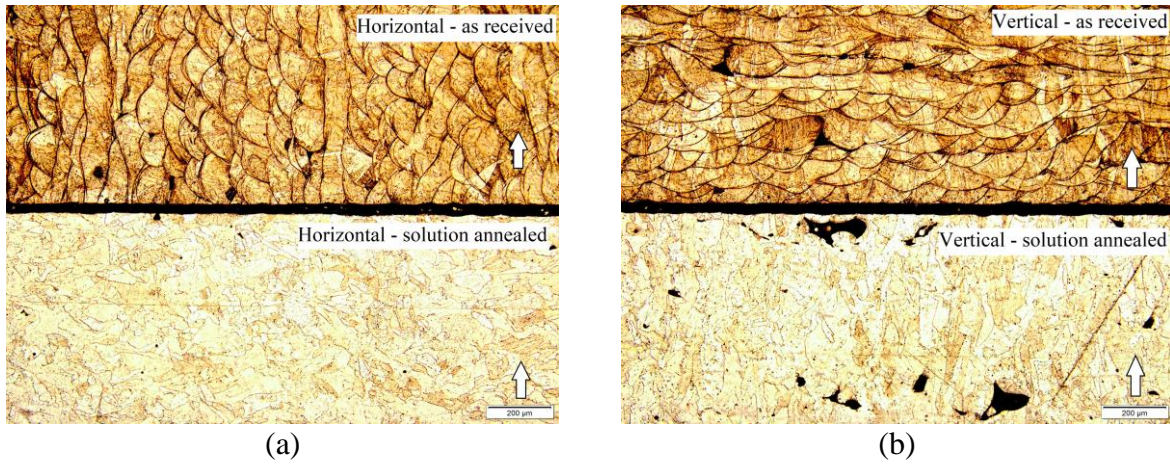


Fig. 2: Microstructure of (a) horizontally (b) vertically built specimens (arrows show specimen axial direction)

Results and discussion

The particular creep curves for all three selected stress levels are shown in Fig. 3. There is an obvious difference between as received and annealed specimens creep curves, the annealed steel performs slightly worse. The overall creep test results in Fig. 4 show excellent creep properties of the SLM. The orientation of the specimens plays minor role in as received state. In the solution annealed state the horizontal direction seems better than vertical. However, most 3D printed specimens perform better than the conventional steel tested in [7,8].

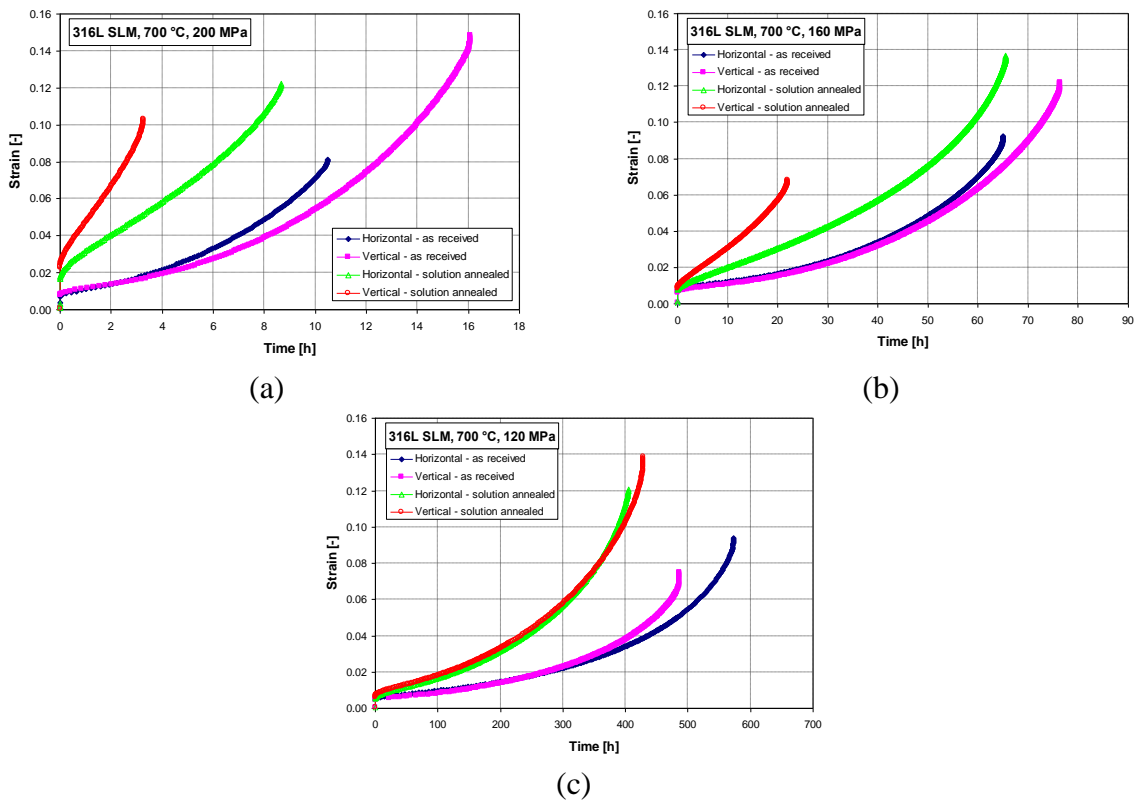


Fig. 3: Creep curves for all tested conditions

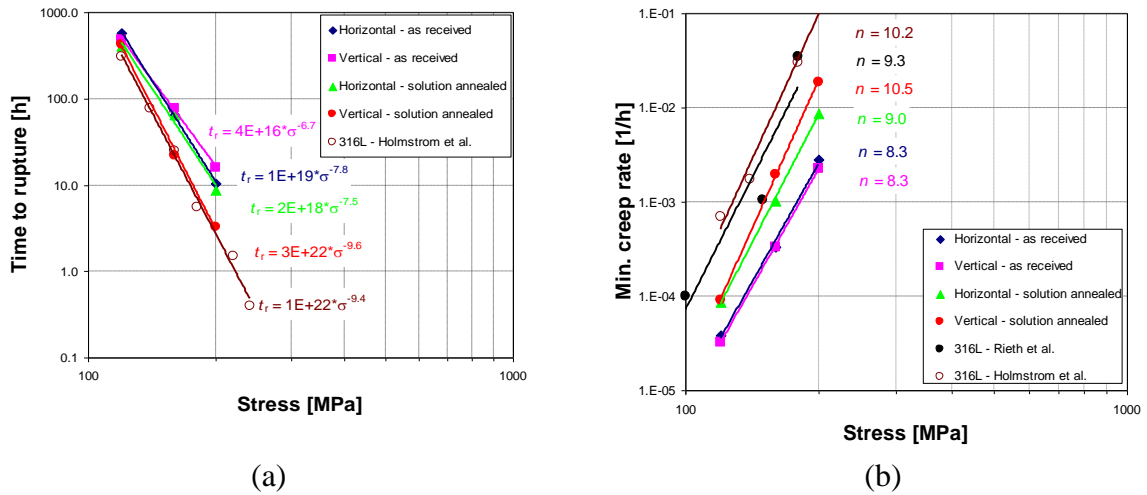


Fig. 4: Creep rupture time (a) and minimum creep rate (b) dependence on applied stress at 700 °C

With lower stress σ and higher time to rupture t_r there is a tendency to receive comparable results with the conventionally prepared steel, as shown in Fig. 4a, but the minimum creep rates still remain notably lower for 3D printed steel which is obvious from Fig 4b. The stress exponent n is comparable or slightly lower for SLM steel compared to conventional steel.

Fractographs after creep in Fig. 5 show ductile fracture with quite limited necking of the as received specimens. There are marked areas of porosity (by the yellow line) that are more frequent and have larger areas on the horizontal specimen in Fig. 5a compared to vertical in Fig. 5b. Vertical specimen has more necking, but at lower stresses, there is no difference. The rupture strains are comparable for all four groups of specimens, which is obvious from the creep curves in Fig. 3. Some scatter in creep ductility is natural. The details of the fracture surfaces near the pores with remaining powder are shown in Fig. 6.

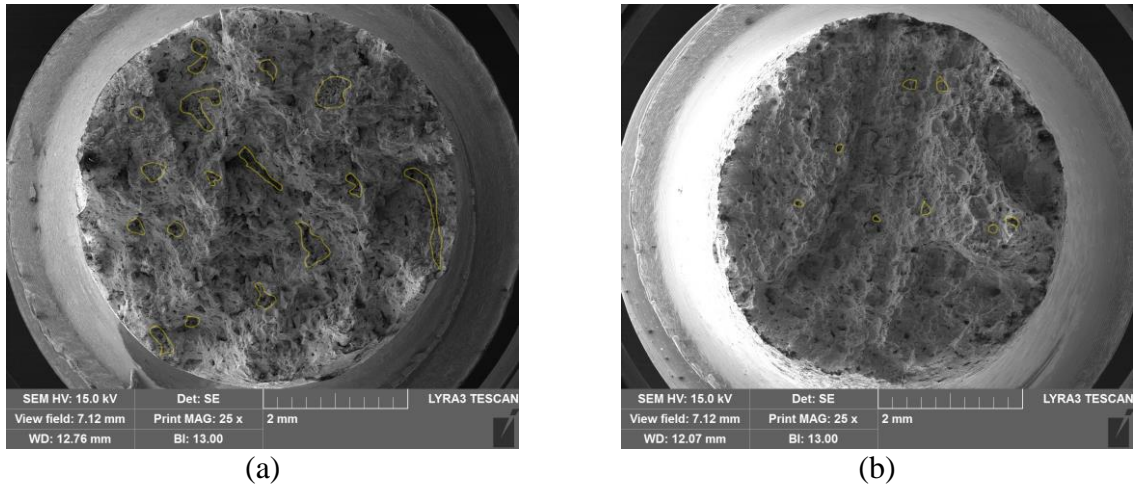


Fig. 5: Fracture surfaces of tests at 200 MPa, (a) horizontal, $t_r = 10.5$ h, (b) vertical, $t_r = 16.1$ h

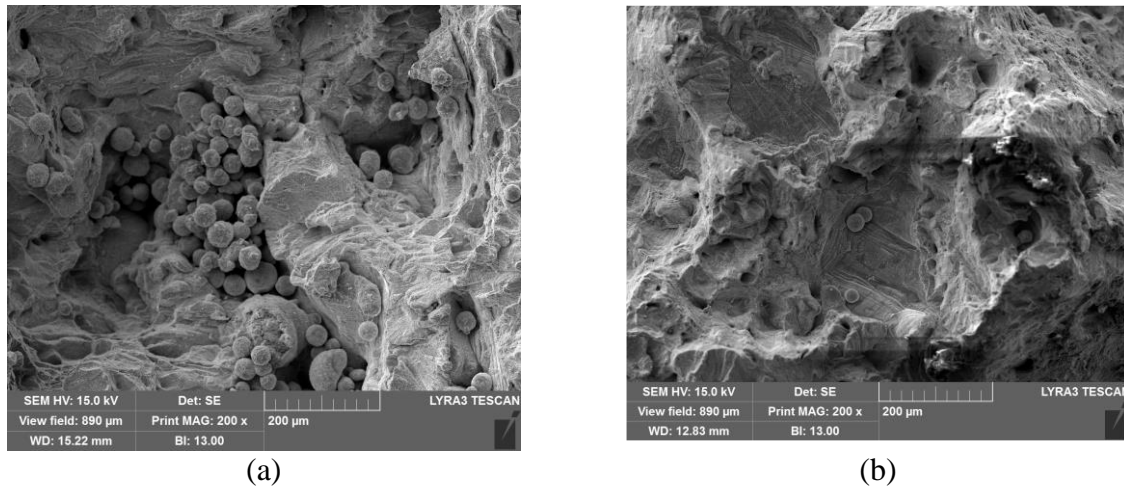


Fig. 6: Detail of fracture near pores with unmelted powder of tests at 200 MPa, (a) horizontal, $t_r = 10.5$ h, (b) vertical, $t_r = 16.1$ h

Despite higher porosity, the better creep performance of 3D printed steel can be attributed to its advantageous microstructure. The microstructural defects and inhomogeneities introduced by SLM can in reality act as hardening objects (similar as precipitates or dislocations) and at the same time as the nucleation sites for the creep damage. One can expect that the rather homogeneously distributed SLM defects cause a significant hardening against dislocation motion and the dominant creep strain is mainly due to cavitation and fracture processes. This idea is supported by the fact of very small primary creep strain. It has to be still verified by detailed microstructure analysis of the crept specimens.

However, longer-term (up to 10 kh) creep behaviour of standard and sub-sized specimens should be further studied in order to assess the high-temperature performance of thin walled structures that might be more sensitive to manufacturing porosity than standard specimens. The microstructure analyses after creep are still under investigation.

Conclusions

In overall the 3D printed 316L stainless steel shows very good short-term creep properties superior to conventional steel. There is not any significant difference in creep performance between the horizontal or vertical direction of printing. Since both studied directions show similar results, the steel can be considered from a creep point of view as isotropic. The solution annealing leads to softening of the steel, higher minimum creep rates and lower times to rupture, which are still comparable or better than of conventionally produced steel.

Acknowledgments

This manuscript has been completed in association with project reg. no. CZ.02.1.01/0.0/0.0/17_049/0008407 financed by Structural Funds of the European Union and within the project TN01000024 financed by The Technology Agency of the Czech Republic.

References

- [1] M. Kraus, V. Mareš, Properties of AISI 316 steel prepared by SLM method, in: Proceedings of New Methods of Damage and Failure Analysis of Structural Parts, 2018, Ostrava, Czech Republic <http://konference.fmt.vsb.cz/work2018/abstracts/Kraus.pdf>.
- [2] R. Halama, M. Pagáč, Z. Paška, P. Pavlíček, X. Chen, Ratcheting Behaviour of 3D Printed and Conventionally Produced SS316L Material, in: Proceedings of the ASME 2019 Pressure Vessels & Piping Conference PVP2019, , San Antonio, TX, USA, 2019, paper number PVP2019-93384.
- [3] P.R. Barrett, T. Hassan, A unified constitutive model in simulating creep strains in addition to fatigue responses of Haynes 230, *Int. J. Solid. Struct.* 185-186 (2020) 394–409.
- [4] K.I. Kourousis, D. Agius, C. Wang, A. Subic, Constitutive modeling of additive manufactured Ti-6Al-4V cyclic elastoplastic behaviour, *Tech. Mech.* 36 (2016) 57–72.
- [5] H.P. Mahajan, T. Hassan, Finite element analysis of printed circuit heat exchanger core for creep and creep-fatigue responses, in: Proceedings of the ASME 2019 Pressure Vessels & Piping Conference PVP2019, San Antonio, TX, USA, 2019 paper number PVP2019-93416.
- [6] J. Hajnys, M. Pagac, O. Kotera, J. Petru, S. Scholz, Influence of Basic Process Parameters on Mechanical and Internal Properties of 316L Steel in SLM Process for Renishaw AM400. *MM Sci. J.* 2019 (1) 2790–2794.
- [7] S. Holmström, Y. Li, P. Dymacek, E. Vacchieri, S.P. Jeffs. R.J. Lancaster, D. Omacht, Z. Kubon, E. Anelli, J. Rantalla, A. Tonti, S. Komazaki, Naveena, M. Bruchausen, R.C. Hurst, P. Hähner, M. Ruchardson, D. Andres, Creep strength and minimum strain rate estimation from Small Punch Creep tests, *Mater. Sci. Eng. A* 731 (2018) 161–172.
- [8] M. Rieth, A. Falkenstein, P. Graf, S. Heger, U. Jäntschi, M. Klimiankou, E. Materna-Moris, H. Zimmermann, Creep of the Austenitic Steel 316L(N) Experiments and models, report FZKA 7065, Nov. 2004, Forschungszentrum Karlsruhe.